Solar treatment (H_2O_2, TiO_2-P25 and GO-TiO_2 photocatalysis, photo-Fenton) of organic micropollutants, human pathogen indicators, antibiotic resistant bacteria and related genes in urban wastewater

Nuno F.F. Moreira[1,2], Carlos Narciso-da-Rocha[3], M. Inmaculada Polo-López[4], Luisa M. Pastrana-Martínez[1], Joaquim L. Faria[1], Célia M. Manaia[3], Pilar Fernández-Ibáñez[4,5,*], Olga C. Nunes[2], Adrián M.T. Silva[1,*]

[1]*Laboratory of Separation and Reaction Engineering - Laboratory of Catalysis and Materials (LSRE-LCM), Faculdade de Engenharia, Universidade do Porto, Rua Dr. Roberto Frias, 4200-465 Porto, Portugal*

[2]*LEPABE – Laboratory for Process Engineering, Environment, Biotechnology and Energy, Faculdade de Engenharia, Universidade do Porto, Rua Dr. Roberto Frias, 4200-465 Porto, Portugal*

[3]*Universidade Católica Portuguesa, CBQF - Centro de Biotecnologia e Química Fina – Laboratório Associado, Escola Superior de Biotecnologia, Rua Arquiteto Lobão Vital, Apartado 2511, 4202-401 Porto, Portugal*

[4]*Plataforma Solar de Almeria – CIEMAT, P.O. Box 22, 04200 Tabernas, Almeria, Spain*

[5]*Nanotechnology and Integrated BioEngineering Centre, School of Engineering, University of Ulster, Newtownabbey, Northern Ireland, BT37 0QB, United Kingdom*

*Corresponding authors e-mail addresses:

adrian@fe.up.pt (A.M.T. Silva); p.fernandez@ulster.ac.uk (P. Fernández-Ibáñez).

Abstract

Solar-driven advanced oxidation processes were studied in a pilot-scale photoreactor, as tertiary treatments of effluents from an urban wastewater treatment plant. Solar-H_2O_2, heterogeneous

photocatalysis (with and/or without the addition of H_2O_2 and employing three different photocatalysts) and the photo-Fenton process were investigated. Chemical (sulfamethoxazole, carbamazepine, and diclofenac) and biological contaminants (human pathogen indicators, their antibiotic resistant counterparts, 16S rRNA and antibiotic resistance genes), as well as the whole bacterial community, were characterized.

Heterogeneous photocatalysis using TiO_2-P25 and assisted with H_2O_2 (P25/H_2O_2) was the most efficient process on the degradation of the chemical organic micropollutants, attaining levels below the limits of quantification in less than 4 hours of treatment (corresponding to Q_{UV} < 40 kJ L^{-1}). This performance was followed by the same process without H_2O_2, using TiO_2-P25 or a composite material based on graphene oxide and TiO_2.

Regarding the biological indicators, total faecal coliforms and enterococci and their antibiotic resistant (tetracycline and ciprofloxacin) counterparts were reduced to values close, or beneath, the detection limit (1 CFU 100 mL^{-1}) for all treatments employing H_2O_2, even upon storage of the treated wastewater for 3-days. Moreover, P25/H_2O_2 and solar-H_2O_2 were the most efficient processes in the reduction of the abundance (gene copy number per volume of wastewater) of the analysed genes. However, this reduction was transient for 16S rRNA, *intI1* and *sul1* genes, since after 3-days storage of the treated wastewater their abundance increased to values close to pre-treatment levels. Similar behaviour was observed for the genes *qnrS* (using TiO_2-P25), $bla_{CTX\text{-}M}$ and bla_{TEM} (using TiO_2-P25 and TiO_2-P25/H_2O_2). Interestingly, higher proportions of sequence reads affiliated to the phylum *Proteobacteria* (*Beta*- and *Gammaproteobacteria*) were found after 3-days storage of treated wastewater than before its treatment. Members of the genera *Pseudomonas, Rheinheimera* and *Methylotenera* were among those with overgrowth.

Keywords: Solar advanced oxidation processes; urban wastewater; human pathogen indicators; antibiotic resistance genes; bacterial community composition.

1. Introduction

Conventional urban wastewater treatment plants (UWWTPs) are not specifically designed for the removal of organic micropollutants, neither for disinfection which considers the inactivation of bacteria that can contribute to the spread of antibiotic resistant bacteria (ARB) and antibiotic resistant genes (ARG) into the environment. These contaminants can reach the natural waters, such as surface and ground waters that are serving as drinking water sources (Fatta-Kassinos et al. 2011, Manaia et al. 2016). Moreover, the continuous disposal of antibiotics and related products into the environment can lead to the development and proliferation of ARB, decreasing the efficiency of these antibiotics when supplied to human and animals (Rizzo et al. 2013, Ferro et al. 2016). Since high bacterial density can be found in effluents of UWWTPs (i.e., bacterial cells are close to each other), horizontal gene transfer and selection of ARB can be considered important mechanisms for ARG enrichment (Davison 1999). The dissemination of these contaminants urges the development of new technologies able to improve the simultaneous removal of organic micropollutants and microorganisms of concern.

Advanced oxidation processes (AOPs) are conceptually based on the generation of the highly reactive hydroxyl radicals ($HO^{\bullet}$), but other reactive species can also be formed. AOPs have been widely studied, mainly with synthetic matrices, and they are seen as viable solutions for the removal of organic micropollutants from urban wastewaters (Ribeiro et al. 2015). Additionally, the formed radicals can also act as disinfectant species leading to effective reduction of high bacterial loads (Moreira et al. 2016, Malato et al. 2009, Sousa et al. 2017, Polo-López et al. 2014, Pablos et al. 2013, Yang et al. 2014). The operating cost of AOPs is one of its main drawbacks holding-off their application. In the case of photo-driven AOPs, sunlight technologies are being developed in an effort to decrease the treatment cost. For instance, solar disinfection showed high efficiency on the reduction of microbial loads, and its efficiency can be increased by the addition of photocatalysts or some chemical agents (Dunlop et al. 2010, Ferro et al. 2015, Fiorentino et al. 2015). In a recent study (Becerra-Castro et al. 2016), we have shown that oxidation processes (such as $UV_{254\ nm}$,

ozonation and photocatalytic ozonation) might have the potential to act selectively over some bacterial groups. In that bench-scale study, irrespective of the type of treatment used, after 3-days storage the bacterial community was characterized by higher proportions of *Proteobacteria* (*Gamma*- and *Betaproteobacteria*) than those observed in non-treated wastewater. This is an example of bacterial community disturbance induced by disinfection, which may affect negatively the biological quality of the final stream.

The present study aims at comparing the efficiency of different solar-driven AOPs on the removal of micropollutants and disinfection of a secondary effluent of an UWWTP. Solar-H_2O_2, heterogeneous photocatalysis (with and/or without the addition of H_2O_2) and the photo-Fenton process were tested using a pilot-plant compound parabolic collector (CPC) solar photoreactor. For the first time, the performance of each process was assessed based on the removal efficiency of organic contaminants and ARB&ARG, as well as on the changes of the bacterial community composition. Microbial characterization was performed before treatment, after 5 hours of treatment and after 3-days storage of treated wastewater at room temperature. Thus, the simultaneous removal of chemical and biological contaminants by using solar-driven AOPs at pilot-scale and considering possible changes in the bacterial community, which can affect the water quality, is the main novelty of the present work.

2. Materials and methods

2.1 Chemicals and materials

Degussa (Aeroxide) TiO_2-P25 catalyst from Evonik Corporation (hereafter referred to as P25) and a composite consisting of TiO_2 and 4.0 wt.% of graphene oxide (GO-TiO_2) – respective preparation method and characterization described elsewhere (Pastrana-Martínez et al. 2012) – were used to conduct heterogeneous photocatalytic experiments. For comparative purposes, bare TiO_2 was also prepared following the same method used for GO-TiO_2, but without the addition of GO (hereafter referred to as TiO_2). The H_2O_2 30% (w/v) solution, analytical grade sulphuric acid (H_2SO_4, 98%),

bovine liver catalase and ferrous sulphate heptahydrate ($FeSO_4 \cdot 7H_2O$) were obtained from Riedel-de Haën (Germany), Merk (Germany), Sigma-Aldrich (USA) and PANREAC (Spain), respectively. Carbamazepine (CBZ), sulfamethoxazole (SMX) and diclofenac (DFC) were all high-purity grade (>99%), and purchased from Sigma-Aldrich (Spain). Stock solutions of each individual compound were dissolved at 2.5 g L^{-1} in methanol due to water solubility limitations. Required amounts of stock solutions were directly loaded into the CPC pilot reactor to obtain the initial concentration of 100 µg L^{-1} of each organic micropollutant in urban wastewater samples. Methanol (J.T.Baker) and acetonitrile (Sigma-Aldrich) were HPLC-grade. Ultrapure water was supplied by a Milli-Q water system.

2.2 Municipal wastewater treatment plant samples

All solar-driven treatments were carried out using urban wastewater samples collected (every day in batches of 60 L) after the secondary treatment from the UWWTP of El Bobar (Almería, Spain), and stored at 4 ºC no more than 2 hours before solar experiments. The UWWTP uses conventional activated sludge plus decantation as secondary treatment. In 2015, it produced an average of secondary effluent daily flow of ca. 33,000 m^3, with a capacity of 100,000 inhabitant-equivalent. The main physicochemical characteristics of the effluent, including turbidity, pH, conductivity, dissolved inorganic carbon (DIC), dissolved organic carbon (DOC) and inorganic ions concentration, are listed in Table 1.

2.3 Pilot scale CPC photoreactor and solar experiments

All the solar-driven oxidation processes were performed in a pilot-scale CPC photoreactor, at Plataforma Solar de Almeria (PSA), Spain (37°84'N and 2°34'W), on sunny days between June and August 2015, with a duration of 5 hours. The configuration of the CPC photoreactor is described elsewhere (Rodríguez-Chueca et al. 2014); it allows the optimal collection of solar radiation (direct and diffuse) and high removal rates of chemical and biological contaminants

(Booshehri et al. 2017, Malato et al. 2013). The CPC photoreactor tube module, tilted at an angle of 37º relative to the horizontal plane, is connected to a recirculation tank and a centrifugal pump. The water flow rate was set at 10 L min^{-1}. The total volume of the photoreactor was 20 L, while the illuminated volume and the irradiated collector surface area were 15 L and 1 m^2, respectively. In heterogeneous photocatalysis (P25, TiO_2 and GO-TiO_2) a catalyst load of 200 mg L^{-1} was used. In photo-Fenton (Fe^{2+}/H_2O_2), ferrous sulphate heptahydrate was used as source of 10 mg L^{-1} of Fe^{2+}. In H_2O_2 assisted processes (H_2O_2, Fe^{2+}/H_2O_2, P25/H_2O_2 and GO-TiO_2/H_2O_2), the initial concentration of H_2O_2 was 20 mg L^{-1} reached by adding the H_2O_2 30% (w/v) solution. The catalyst and H_2O_2 concentrations were selected considering the optimization done in our previous studies with solar-driven oxidation processes (Polo-López et al. 2014, Fernández-Ibáñez et al. 1999). Immediately after the collection of a sample, residual H_2O_2 was eliminated by adding a freshly prepared solution of bovine liver catalase (0.1 g L^{-1}) in a ratio 0.1/5.0 (v/v). Photolysis (Blank) assays were performed to study the effect of solar radiation without the addition of any catalyst or reactant.

Besides the experimental time, the accumulated solar UVA energy received in the solar reactor per unit of treated water volume (Q_{UV}, kJ L^{-1}) was considered for comparison of the treatment efficiencies (Malato et al. 2009) and calculated using Eq. (1):

$$Q_{UV,n} = Q_{UV,n-1} + \frac{\Delta t_n \overline{UV}_{G,n} A_r}{V_t}; \Delta t_n = t_n - t_{n-1} \quad (1)$$

where $UV_{G,n}$ is the global UV irradiance (W m^{-2}) averaged during exposure time; t_n the exposure time (s); V_t the total reactor volume (L); and A_r the illuminated reactor surface (m^2).

A global UVA (300–400 nm, Model CUV4, Kipp & Zonen, Netherlands) pyranometer tilted 37° was used to measure the solar radiant UVA rate incident (W m^{-2}) as described elsewhere (Rodríguez-Chueca et al. 2014). The average value of solar UVA irradiance was 40 W m^{-2}.

Before treatment, the CPC photoreactor was covered by an opaque sheet while the wastewater and reagents were added to the reactor and recirculated during 15 min to guarantee homogenisation.

156 Samples were collected each hour over the treatment. During this period, temperature (Checktemp,
157 Hanna instruments, Spain) and pH (multi 720, WTW, Germany) were measured. The temperature
158 of the wastewater varied from 16.6 ± 1.5 ºC to 43.2 ± 4.2 ºC.
159
160 **Table 1.** Chemical characterization of the secondary wastewater from the UWWTP. Values are the average
161 of four independent assays and errors represents standard deviations.

Secondary effluent characterisation				
Turbidity (NTU)	5.3 ± 3.1		PO_4^{3-} (mg L^{-1})	12.4 ± 6.1
pH	7.5 ± 0.2		SO_4^{2-} (mg L^{-1})	74.5 ± 15.6
Conductivity (µS cm^{-1})	1780 ± 63		Br^- (mg L^{-1})	2.7 ± 0.7
DIC† (mg L^{-1})	55 ± 30		Na^+ (mg L^{-1})	199 ± 6
DOC† (mg L^{-1})	19 ± 4		Cl^- (mg L^{-1})	368 ± 18
NH_4^+ (mg L^{-1})	35.3 ± 25.5		K^+ (mg L^{-1})	25.6 ± 1.8
NO_3^- (mg L^{-1})	68.6 ± 64.5		Mg^{2+} (mg L^{-1})	35.3 ± 2.6
NO_2^- (mg L^{-1})	1.8 ± 1.0		Ca^{2+} (mg L^{-1})	74.9 ± 3.2

162 †DIC: dissolved inorganic carbon; †DOC: dissolved organic carbon.
163
164 *2.4 Chemical analysis*
165 High performance liquid chromatography (HPLC) was used to analyze the evolution of the target
166 organic micropollutants using an apparatus from Agilent Technologies (series 1260, Palo Alto, CA,
167 USA), equipped with a diode array detector (UV-DAD) and a C-18 column. The mobile phase
168 consisted of 90% formic acid aqueous solution at 25 mM and 10% acetonitrile. A linear gradient
169 was used from 10% to 85% of acetonitrile during 13 min at a flow rate of 1 mL min^{-1}. The injection
170 volume was set at 100 µL. Before injection, samples were filtered through a 0.2 µm syringe-driven
171 filter, and afterwards the filter was washed with 1 mL of acetonitrile to remove the adsorbed
172 compounds. CBZ, SMX and DFC were selected as model organic micropollutants since they have
173 been frequently found in aquatic environments, including wastewater, surface and groundwater and

even in drinking water (Barbosa et al. 2016). The detection wavelength values were 267 nm for both CBZ and SMX, and 273 nm for DFC. The limits of quantification (LOQ) were 4.7, 6.2 and 4.1 µg L^{-1} for CBZ, SMX and DFC, respectively.

DX-600 and DX-120 (Dionex Corporation, Sunnyvale, CA) equipments were used for quantification of anions and cations, respectively. DOC and DIC measurements were performed using a 5050 A TOC (Shimadzu Corporation, Kyoto, Japan) analyzer, after sample filtration using 0.2 µm syringe filters. Turbidity was determined with a turbidimeter (Model 2100N, Hach, USA). The H_2O_2 concentration was determined by a spectrometric method, as described elsewhere (Polo-López et al. 2011), and the Fe^{2+} concentration by the ISO 6332 method. Natural iron was not detected in any of the urban wastewater samples by using this method, i.e. a spectrophotometric technique with phenanthroline/acetic acid (UV–Vis measurements, limit of detection 0.05 mg L^{-1}).

2.5 Microbiological cultivation, DNA extraction, qPCR and bacterial community analysis

To assess the disinfection efficiency, cultivable indicator bacteria, targeted ARB and selected ARGs were quantified before and immediately after the 5 hours-treatment, and after 3-days of storage of treated wastewater at room temperature. The abundance of faecal coliforms, enterococci and their tetracycline and ciprofloxacin resistant counterparts was assessed by using the membrane filtration method. After serial 10-fold dilutions in sterile saline solution (0.85% NaCl), 100 mL of each dilution was filtered through cellulose membrane filters (0.22 µm porosity; Whatman, UK). The filtering membranes were incubated on selective media for each target bacterial groups - membrane Faecal Coliforms agar (m-FC) (Difco, 30 °C, 24 hours) for faecal coliforms, and Slanetz & Bartley agar (S&B) (Difco, 30 °C, 48 hours) for enterococci. In addition, the prevalence of ARB was assessed in the same media supplemented with tetracycline (Fluka, 16 mg L^{-1}) and ciprofloxacin (Applichem, 1 mg L^{-1}). The antibiotic stock solutions were sterilized by filtration (0.2 µm syringe driven-filters). For culture-independent assays, a volume of 250 mL of each sample (before and after the 5 hours treatment, and after 3-days of storage) was filtered through

polycarbonate membranes (0.22 µm porosity; Whatman, UK). DNA was extracted using the commercial kit PowerWater® DNA Isolation (MO BIO Laboratories, Inc., USA) and stored at -20 °C. These extracts were used for quantitative PCR (qPCR) of samples collected before treatment, immediately after treatment, and after 3-days of storage, and also for the bacterial community analysis, in this case except for the samples collected immediately after treatment, due to DNA scarcity. The qPCR (StepOne™ Real-Time PCR System; Life Technologies, Carlsbad, CA) assays were performed according to the conditions shown in Table 2, as described elsewhere (Narciso-da-Rocha et al. 2014).

Table 2. Target genes and conditions used in qPCR assays.

Target gene	Primers (sequence) Reference	Conditions	Efficiency (%)	Reference
16S rRNA	1114F (CGGCAACGAGCGCAACCC) 1275R (CCATTGTAGCACGTGTGTAGCC) *Escherichia coli* - ATCC 25922	95 °C for 10 min (1 cycle) 95 °C for 15 s, 55 °C for 20 s and 72 °C for 10 s (35 cycles)	100	(Denman and McSweeney 2006)
bla$_{TEM}$	blaTEM-F (TTCCTGTTTTTGCTCACCCAG) blaTEM-R (CTCAAGGATCTTACCGCTGTTG) *Escherichia coli* - A2FCC14	95 °C for 10 min (1 cycle) 95 °C for 15 s, 60 °C for 30 s and 72 °C for 10 s (40 cycles)	96	(Bibbal et al. 2007)
intI1	intI1-F (CCTCCCGCACGATGATC) intI1-R (TCCACGCATCGTCAGGC) *Escherichia coli* - A2FCC14	95 °C for 10 min (1 cycle) 95 °C for 15 s, 55 °C for 30 s and 72 °C for 10 s (40 cycles)	94	(Goldstein et al. 2001)
*qnr*S	qnrSrtF11 (GACGTGCTAACTTGCGTGAT) qnrSrtR11 (TGGCATTGTTGGAAACTTG) *Enterobacter cloacae* - S1+	95 ºC for 5 min (1 cycle) 95 ºC for 15 s and 60 ºC for 1 min (40 cycles)	95	(Marti and Balcázar 2013)
*sul*1	sul1-FW (CGCACCGGAAACATCGCTGCAC) sul1-RV (TGAAGTTCCGCCGCAAGGCTCG) *Achromobacter sp.*	95 ºC for 5 min (1 cycle) 95 ºC for 15 s and 60 ºC for 1 min (40 cycles)	94	(Pei et al. 2006)
*van*A	vanA3FP (CTGTGAGGTCGGTTGTGCG) vanA3RP (TTTGGTCCACCTCGCCA) *Enterococcus faecalis* - H1EV23	95 ºC for 5 min (1 cycle) 95 ºC for 15 s and 60 ºC for 1 min (40 cycles)	98	(Volkmann et al. 2004)
bla$_{CTX-M}$	CTXM-FW (CTATGGCACCACCAACGATA) CTXM-RV (ACGGCTTTCTGCCTTAGGTT) *Escherichia coli* - A2FC14	95 ºC for 10 min (1 cycle), 95 ºC for 15 s and 60 ºC for 1 min (40 cycles)	94	(Marti et al. 2014)

The bacterial community composition was analysed based on the hypervariable V3/V4 region (forward primer Bakt_341F 5′-CCTACGGGNGGCWGCAG-3′ and reverse Bakt_805R 5′-GACTACHVGGGTATCTAATCC-3') of 16S rRNA gene Illumina sequencing (Genoinseq, Cantanhede, Portugal). Nucleotide sequencing data were processed and analyzed using the QIIME pipeline (Caporaso et al. 2010a). Briefly, sequences shorter than 250 bp and with average quality scores lower than 25 were eliminated, and bases with average quality lower than 25 in a window of 5 bases, were trimmed using the software PRINSEQ (Schmieder and Edwards 2011). Chimeric sequences were identified and removed using USEARCH v6.1 (Edgar 2010). Free-chimeric sequences were further grouped into operational taxonomic units (OTUs) using USEARCH v6.1 (Edgar 2010) with a phylotype threshold of ≥ 97% sequence similarity and were taxonomically assigned using QIIME default values. The sequences comprising each OTU were aligned using PyNAST (Caporaso et al. 2010b) and were taxonomically classified using Greengenes Database version 13_8 (updated: August 2013) (DeSantis *et al.* 2006). As a variable number of sequences was obtained between samples, the alpha diversity indices Shannon, phylogenetic diversity (PD) whole tree, and Simpson were calculated after rarefying to 54,771 sequences *per* sample (value of the smallest dataset) (Shannon and Weaver 1963, Simpson 1949, Faith 1992). The cumulative sum scaling (CSS) normalization procedure was applied to the sequence data to assess the beta diversity patterns (Paulson et al. 2013). The weighted UniFrac metric distances (Lozupone and Knight 2005) were calculated in the QIIME pipeline and the results shown as Principal Coordinates Analysis (PCoA) biplots that include the position of the ten most prevalent bacterial classes. Correlations between the relative abundance of populations at different taxonomic levels were analyzed using the statistics software STAMP v2.1.3 (Parks et al. 2014).

3. Results and discussion

3.1 Degradation of organic micropollutants

The evolution of the concentrations of targeted organic micropollutants (i.e., CBZ, SMX and DFC) spiked in urban wastewater under solar-driven oxidation treatments are shown in Fig. 1. Control experiments were performed under the same conditions but without the addition of any catalyst or H_2O_2 (i.e., Blank = photolysis). CBZ and SMX were very resistant upon irradiation in the absence of a catalyst or H_2O_2 (only 20 ± 6% and 17 ± 4% of removal, respectively). In contrast, DFC was efficiently removed by photolysis after 4 hours. This result was expected since the DFC absorption spectrum (not shown) has a tail entering well above the 300 nm (Moreira et al. 2015).

The heterogeneous photocatalysts (P25, TiO_2 and GO-TiO_2), without the addition of H_2O_2, converted the targeted organic micropollutants in the following order of decreasing efficiency: P25 > GO-TiO_2 > TiO_2 (Fig. 1). The high photocatalytic efficiency of GO-TiO_2 on the degradation of different types of organic micropollutants in synthetic matrices has been already demonstrated in our previous studies, namely for: diuron, alachlor, isoproturon and atrazine – pesticides classified by the EU as priority pollutants (Cruz et al. 2017); microcystin-LA – cyanotoxin (Sampaio et al. 2015); bisphenol A – xenoestrogen (Maroga Mboula et al. 2013); diphenhydramine – antihistamine pharmaceutical, and methyl orange – azo dye (Pastrana-Martínez et al. 2012). The GO-TiO_2 photocatalyst has been much more active than P25 under Vis-light illumination, but under near UV-Vis radiation the activity of this type of photocatalysts depends on the target pollutant. The better performance of GO-TiO_2 in comparison to bare TiO_2 has been attributed to the good assembly and interfacial coupling between TiO_2 and GO sheets as well as the respective quenching of photoluminescence (inhibiting charge recombination) (Pastrana-Martínez et al. 2012). In the present study, P25 was the most efficient photocatalyst for the degradation of the organic micropollutants, most probably, because of the large fraction of UV radiation entering the photo-reactor by the CPC mirror configuration.

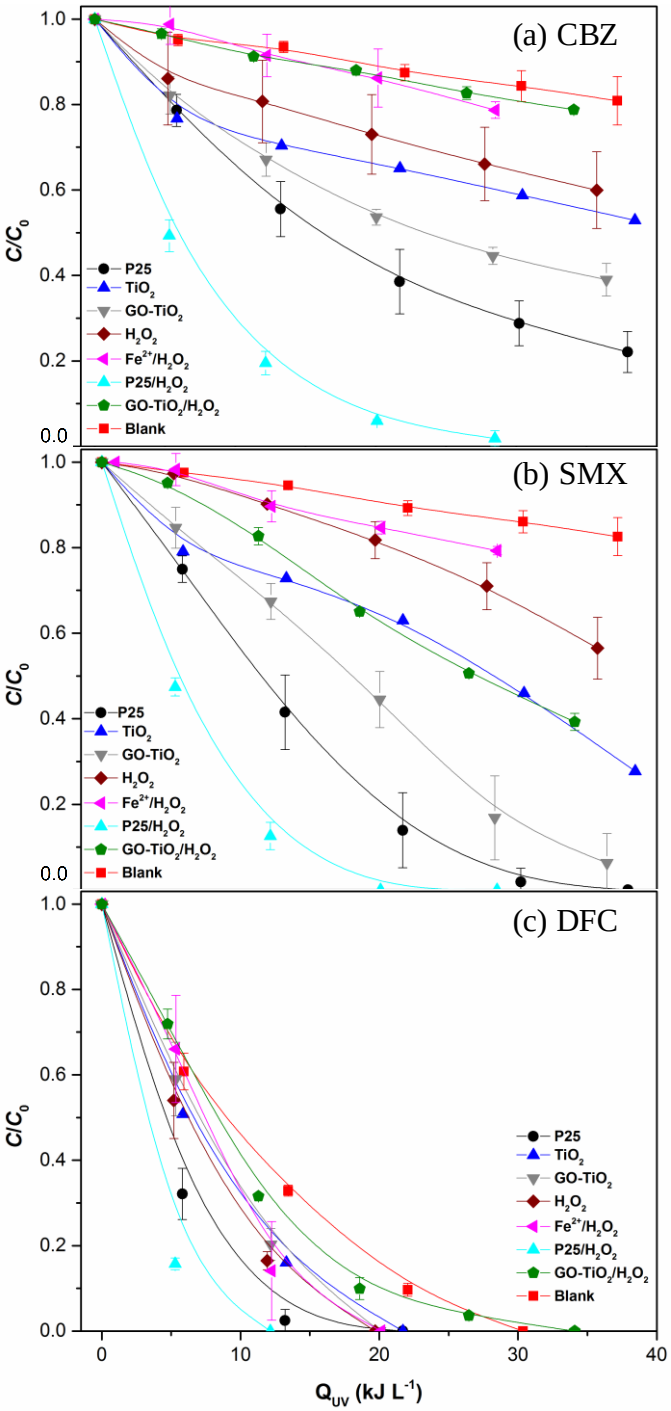

Figure 1. Normalized concentration (C/C_0) of (a) CBZ, (b) SMX and (c) DFC spiked in urban wastewater as function of accumulated energy (Q_{UV}) using different solar-driven treatments. Except for TiO_2, values are the average of four (P25), three (GO-TiO_2, H_2O_2, Fe^{2+}/H_2O_2) and two ($P25/H_2O_2$, GO-TiO_2/H_2O_2, Blank) independent assays. Error bars represent standard deviations.

The addition of H_2O_2 to the P25 photocatalytic system, significantly increased the degradation efficiency of the targeted micropollutants. H_2O_2 captures and reacts with the photoinduced surface

electrons (supressing the electron/hole recombination) and it also reacts with the superoxide radical anions, both pathways leading to the formation of additional hydroxyl radicals (Pablos et al. 2013, Kositzi et al. 2004). There is markedly a competing process, which may be mediated by the active surface of the photocatalyst. Interestingly, the removal efficiency decreased when H_2O_2 was added to the photocatalytic system containing GO-TiO_2. Degradation of GO-TiO_2 may eventually occur, for instance by the H_2O_2 attack to the underlying C-C bonds in the superficial defect sites of GO (Xing et al. 2014).

Solar-H_2O_2 and photo-Fenton processes (Fe^{2+}/H_2O_2) also led to very modest removals of CBZ and SMX (Figs. 1a and b, respectively). One of the downsides of photo-Fenton is the formation of iron sludge due to the precipitation of iron hydroxide at neutral pH. In this work, the pH was adjusted to a circumneutral value (5.5) by using H_2SO_4, which could explain the low photo-Fenton efficiency that is known to be maximized at pH values around 3 (Giannakis et al. 2017, Agulló-Barceló et al. 2013, García-Fernández et al. 2012).

Overall, P25/H_2O_2 followed by the P25 and GO-TiO_2 photocatalytic processes were the best performing treatments for removal of the targeted organic micropollutants. Regarding the mineralization of the organic matter present in the urban wastewater, P25/H_2O_2, solar-H_2O_2, and the photo-Fenton process were the most efficient treatments (DOC removals always around 23 ± 3%), other processes removing no more than ca. 10% of the initial DOC.

3.2 Bacteria inactivation and reactivation

The performance of different solar-driven processes was assessed before and over the treatment, in terms of removal of total faecal coliforms (Fig. 2a), enterococci (Fig. 2c) and respective fraction of resistant populations (Figs. 2b and d). The reduction of the bacterial indicators loads was observed in all the treatments, with the highest inactivation rates leading to values bellow or close the LOD (1 CFU 100 mL^{-1}), for the processes where H_2O_2 was used (H_2O_2, Fe^{2+}/H_2O_2, P25/H_2O_2, GO-TiO_2/ H_2O_2). Among these, and despite the iron precipitation, the photo-Fenton process was

the most efficient treatment on the reduction of resistant and non-resistant faecal coliforms and enterococci (Figs. 2a-d, Fe^{2+}/H_2O_2). However, photo-Fenton showed similar disinfection profiles to solar-H_2O_2 for faecal coliforms (Figs. 2a and b) and to P25/H_2O_2 for enterococci (Figs. 2c and d). These three processes removed those bacteria for Q_{UV} < 30 kJ L^{-1}, suggesting that H_2O_2 plays a major role on disinfection. In contrast, moderate inactivation rates were observed for photolysis (Figs. 2a, b and c, Blank), except for antibiotic resistant enterococci that were reduced to values bellow the LOD (Fig. 2d, Blank). Interestingly, P25/H_2O_2 showed high efficiency on the removal of organic micropollutants and resistant and non-resistant enterococci, whereas the efficiency for inactivation of resistant and non-resistant faecal coliforms was not so high in comparison with solar-H_2O_2.

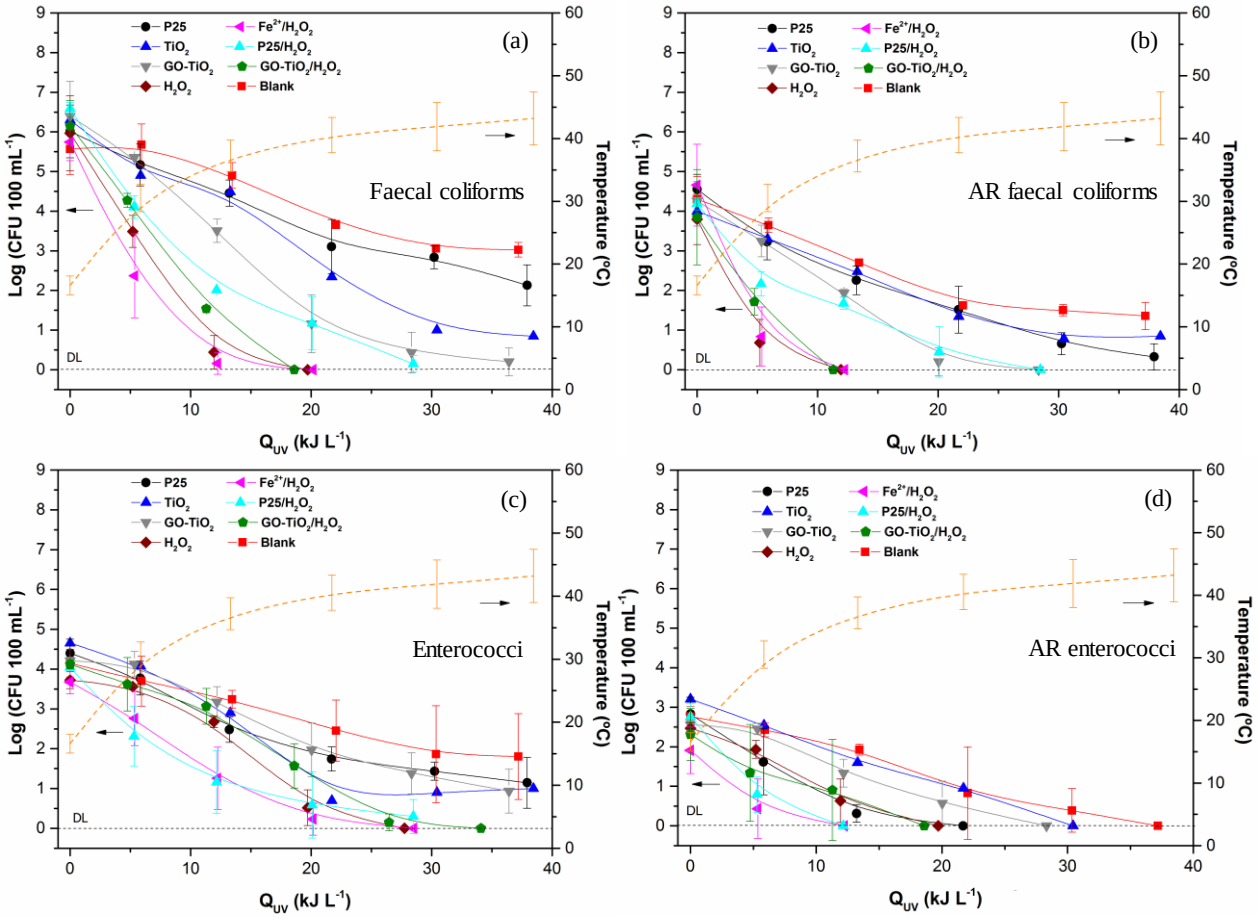

Figure 2. Faecal coliforms (a) and enterococci (c) and their antibiotic resistant counterparts (b, d) inactivation in urban wastewater as function of accumulated energy (Q_{UV}) using different solar-driven treatments. Except for TiO_2, values are the average of four (P25), three (GO-TiO_2, H_2O_2, Fe^{2+}/H_2O_2) and two

309 (P25/H_2O_2, GO-TiO_2/H_2O_2, Blank) independent assays. Error bars represent standard deviations. DL,
310 detection limit.
311
312 The accepted hypotheses and mechanism that explain the inactivation of microorganisms by
313 exposure to solar-H_2O_2 is based on the accumulated damages inside cells by internal cellular injures
314 occurring under sunlight and accelerated in the presence of H_2O_2. It is well accepted that solar
315 radiation produces internal damages affecting different intracellular vital components leading to
316 bacterial death or lack of viability (Aguas et al. 2017). A recent study attributed bacterial
317 inactivation during solar photolysis to the combined effect of intracellular production of reactive
318 oxygen species by UV photons absorption and water temperature increase (Castro-Alférez et al.
319 2017). When H_2O_2 is added, it may diffuse inside bacteria cells promoting additional internal
320 photo-reactions with naturally present iron and other metals via Fenton and Fenton–like reactions,
321 activating, thus, a photo-Fenton cycle under sunlight at intracellular level also (Aguas et al., 2017).
322 Both photo-effects act jointly producing an accelerated disinfection that has been also reported to
323 be very efficient for other types of bacteria, viral indicators, and fungi including, *Escherichia coli*
324 and *Enterococcus faecalis* (Rodríguez-Chueca et al. 2014), *Legionella jordanis* (Polo-López et al.
325 2017), F-specific RNA bacteriophage (Agulló-Barceló et al. 2013), *Fusarium* sp. (Polo-López et
326 al. 2014, Sichel et al. 2009), *Phytophthora capsici* (Polo-López et al. 2013), *Curvularia* sp. (Aguas
327 et al. 2017), and several antimicrobial resistant bacteria (Fiorentino et al. 2015).
328 Although H_2O_2 assisted processes performed better that non-assisted ones, heterogeneous
329 photocatalysis without H_2O_2 also performed quite well on the inactivation of total or resistant
330 populations of faecal coliforms and enterococci. Among these processes, the GO-TiO_2 composite
331 was the most efficient catalyst for the removal of total and resistant populations of faecal coliforms
332 (Figs. 2a and b, GO-TiO_2). The good efficiency of photocatalytic disinfection using this type of
333 composites (but prepared by other methods) and under visible radiation only was already shown in
334 previous studies (Cruz-Ortiz et al. 2017, Fernández-Ibáñez et al. 2015). Its high photocatalytic

activity has been attributed to the improvement in charge separation since GO may promote the electron transfer with TiO_2 particles, acting as an electron bridge, and to the decrease of the bandgap energy of the composite catalysts as well as to an enhancement of the adsorptive properties. These authors concluded that hydrogen peroxide, hydroxyl radicals, and singlet oxygen were the main species involved in the disinfection process under UV–Vis irradiation and only singlet oxygen under visible illumination (Cruz-Ortiz et al. 2017).

Since microbial inactivation, monitored via culture-based methods, can be a transient (Moreira et al. 2016, Zhao et al. 2014, Spuhler et al. 2010), further assays testing the regrowth capacity after 3-days storage of the treated wastewater at room temperature were performed. Bacterial reactivation is influenced by factors such as the storage conditions, temperature, availability of nutrients and the UV dose, among others (Ubomba-Jaswa et al. 2009, Giannakis et al. 2014). The bacterial loads before, after the treatment and after 3-days storage at room temperature are shown in Figs. 3a and b for faecal coliforms and Figs. 3c and d for enterococci. No regrowth was observed in stored wastewater treated by the H_2O_2-assisted processes, and total faecal coliforms and enterococci as well as their ARB counterparts were kept below the detection limit. In stored wastewater treated by heterogeneous photocatalysis without H_2O_2 (P25, TiO_2 and GO-TiO_2), the bacterial loads of these groups were 2 to 3 log values lower than before the treatment. Similar observations were registered for the control (Blank = photolysis). These results indicate the inability of these bacterial groups to recover after the tested solar-driven processes. This can be also explained by the mode of action attributed to solar-H_2O_2 disinfection, where oxidative damages alter the bacteria viability at intracellular level, as proven in the literature (Castro-Alférez et al. 2017). In such report, an EMA-qPCR method for the detection of membrane integrity damages of *L. jordanis* cells under two photo-oxidative processes was used, i.e. solar-H_2O_2 and P25 with solar radiation. It was confirmed the well-accepted mechanism of heterogeneous (P25) photocatalysis via oxidative attacks of the external cell membrane, whereas the mechanism for solar-H_2O_2 was based on internal photochemical reactions. This may explain the results reported

in Fig. 3 on the non-recover capability of ARB when H_2O_2 was used in these treatment processes, while they can regrow when H_2O_2 is not in the media (Castro-Alférez et al. 2017).

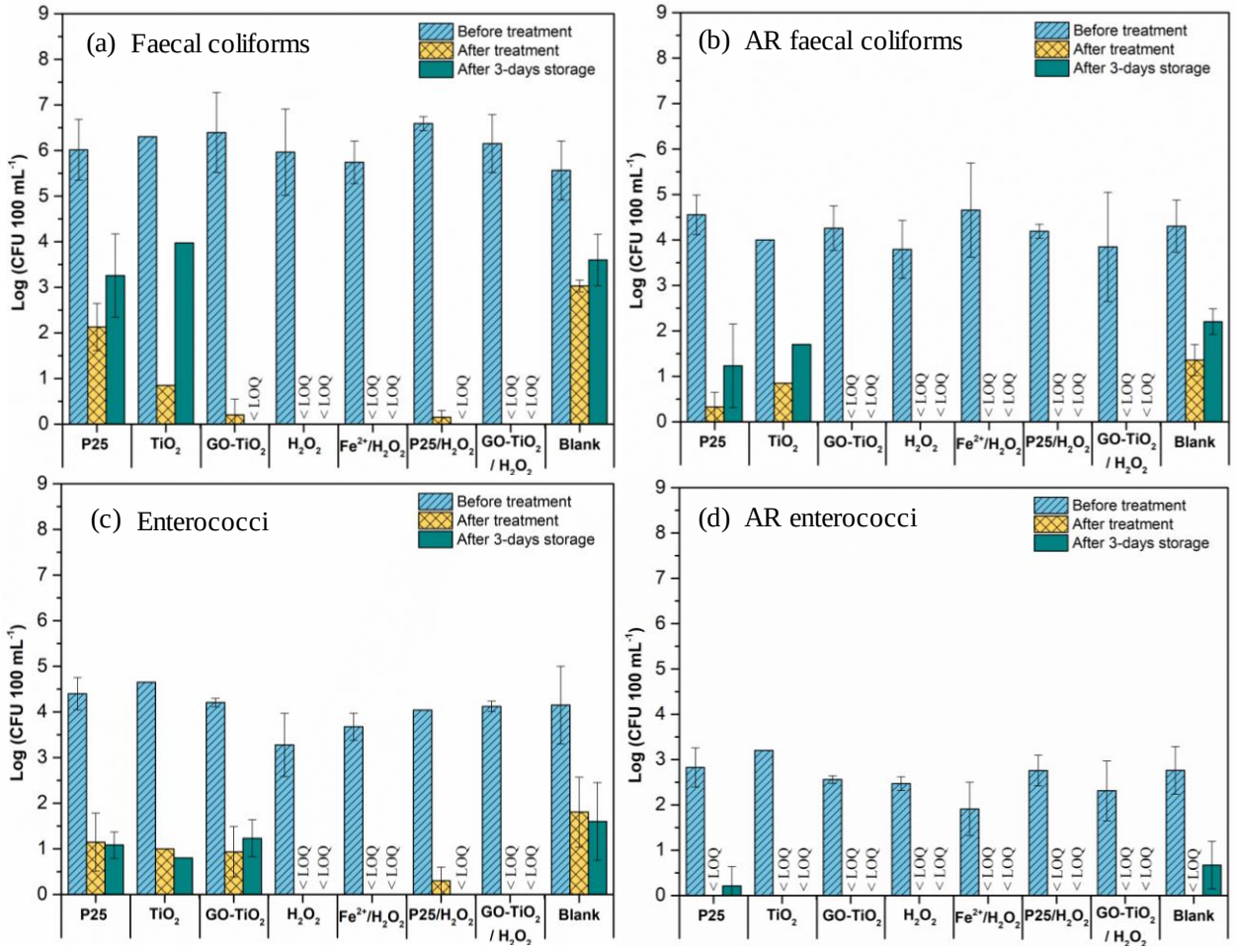

Figure 3. (a) Faecal coliforms and (c) enterococci and their (b, d) antibiotic resistant counterparts counts before, after treatment and after 3-days storage using different solar-driven treatments. Except for TiO_2, values are the average of four (P25), three (GO-TiO_2, H_2O_2, Fe^{2+}/H_2O_2) and two ($P25/H_2O_2$, GO-TiO_2/H_2O_2, Blank) independent assays. Error bars represent standard deviations.

3.3 Effect of disinfection on ARGs and bacterial community composition

Considering that the bacterial community is much more diversified and complex than that assessed based on the cultivation methods used, and that some bacteria may be injured and hence, unable to grow, culture-independent methods were carried out to give additional insights on the disinfection effectiveness of the studied solar-driven processes. Since the main purpose of this work was the

simultaneous removal of chemical and biological contaminants, the processes showing better performance on the degradation of organic micropollutants (i.e., P25/H_2O_2, P25 and GO-TiO_2 photocatalytic processes), disinfection (P25/H_2O_2 and solar-H_2O_2), and also the reference process (photolysis), were selected for further investigation based on culture-independent methods - Fe^{2+}/H_2O_2 was not chosen due to its bad performance for degradation of the organic micropollutants (Fig. 1).

Among the analysed genes (i.e., 16S rRNA, *intI1*, *qnrS*, bla_{CTX-M}, *sul1*, bla_{TEM} and *vanA*), only *vanA* was below the LOD before treatment (not shown). For the other genes, P25/H_2O_2 photocatalysis and solar-H_2O_2 were the most efficient processes (i.e., lower abundance after treatment), both leading to log average reductions of 1-2 values (Fig. 4). However, after 3-days storage, regardless the treatment used, the abundance of 16S rRNA gene, a house keeping gene of prokaryotes, was close or even higher (up to 1 log for P25/H_2O_2) than those found before treatment, suggesting the ability of bacteria to recover after the treatment. Similar results were observed for *intI1* and *sul1* genes, encoding integrase and conferring resistance to sulphonamides, respectively. Among the studied processes, only solar-H_2O_2 and GO-TiO_2 prevented the reactivation of bla_{CTX-M} and bla_{TEM} genes (encoding resistance to beta-lactams) above the pre-treatment levels. For the *qnrS* gene (encoding resistance to quinolones), besides these two processes, also P25/H_2O_2 prevented its reactivation.

The effect of the different treatment processes on the bacterial communities was another aim of this study. Out of the 49 phyla found in freshly collected wastewater (before treatment), *Proteobacteria* (62 ± 7%) and *Bacteroidetes* (10 ± 2%) were, in average (n=8), the most abundant (Fig. 5a, t_0). *Proteobacteria* comprised mainly members of the classes *Beta-* (28 ± 2%), *Gamma-* (20 ± 10%), *Alpha-* (7 ± 2%) and *Deltaproteobacteria* (5 ± 1%). Beside these groups, several other bacterial classes were detected in the freshly collected wastewater in relative abundances ranging from 2 ± 1% to 4 ± 2%; examples are "*Saprospirae*", *Flavobacteriia* and *Bacteroidia*

(*Bacteroidetes*), *Clostridia* (*Firmicutes*), *Planctomycetia* (*Planctomycetes*), *ZB2* (*OD1*) and *TM7-1* (*TM7*). The other identified classes had abundances < 1.3% (Fig. 5a, t_0).

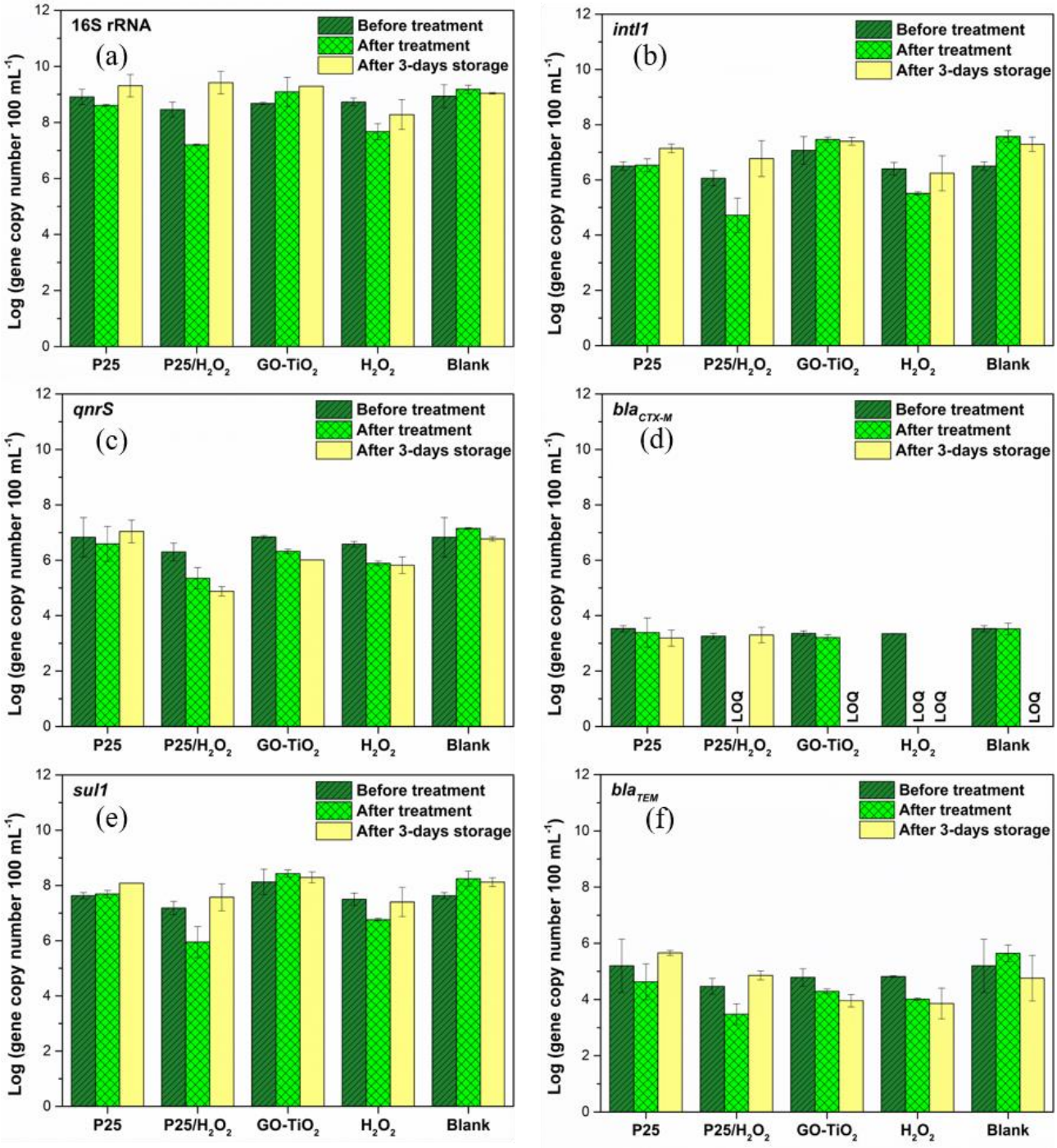

Figure 4. Abundance of target genes before and after treatment, and after 3-days storage at room temperature using different solar-driven treatments: (a) 16S rRNA, (b) *intI1*, (c) *qnr*S, (d) bla_{CTX-M}, (e) *sul*1 and (f) bla_{TEM}. Values are the average of two independent assays. Error bars represent standard deviations.

Regardless of the solar driven process, treatment followed by storage at room conditions led to important bacterial community rearrangements that, in general, had the same pattern. The relative abundance of the members of *Proteobacteria* was higher ($p < 0.01$) in the stored treated wastewater than in the freshly collected wastewater samples, whereas it was lower ($p < 0.01$) for the majority of members of the other phyla (Fig. 5a, t_3). The lower values of the alpha-diversity indices of the stored treated wastewater samples when compared with those of freshly collected wastewater samples (Table 3) corroborate this loss of diversity and equitability. These rearrangements are well depicted in the PCoA biplot, where the bacterial communities of the freshly collected wastewater samples were separated from those treated and stored over axis PC1 (31.0%) (Fig. 6, squares and stars, respectively).

Table 3. Alpha diversity indices of the wastewater samples before (t_0) and after 3-days storage after treatment (t_3) calculated based on the average of 10 rarefaction OTU tables.

Experiment	Time	OTUs No.	Shannon	Simpson	PD whole tree
P25	t_0	3023	7.0	0.95	125.6
P25 *	t_0	3181	8.3	0.99	158.7
P25	**t_3**	3267	6.6	0.92	101.8
P25 *	**t_3**	4010	7.3	0.96	123.8
P25 / H_2O_2	t_0	3353	7.8	0.98	156.7
P25 / H_2O_2 *	t_0	3586	8.1	0.98	164.8
P25 / H_2O_2	**t_3**	2462	6.1	0.93	59.4
P25 / H_2O_2 *	**t_3**	2047	4.9	0.84	58.7
GO-TiO_2	t_0	3425	8.1	0.98	161.2
GO-TiO_2 *	t_0	2687	7.6	0.97	136.3
GO-TiO_2	**t_3**	2419	5.6	0.83	95.5
GO-TiO_2 *	**t_3**	2628	6.5	0.93	92.7
H_2O_2	t_0	3161	7.8	0.98	155.7
H_2O_2 *	t_0	3567	8.1	0.98	166.3
H_2O_2	**t_3**	2179	5.2	0.84	79.4
H_2O_2 *	**t_3**	2595	6.3	0.91	136.2
Blank	t_0	3023	7.0	0.95	125.6
Blank *	t_0	3181	8.3	0.99	158.7
Blank	**t_3**	3487	6.7	0.94	112.4
Blank *	**t_3**	3511	6.3	0.91	111.0

*, indicates a second independent assay.

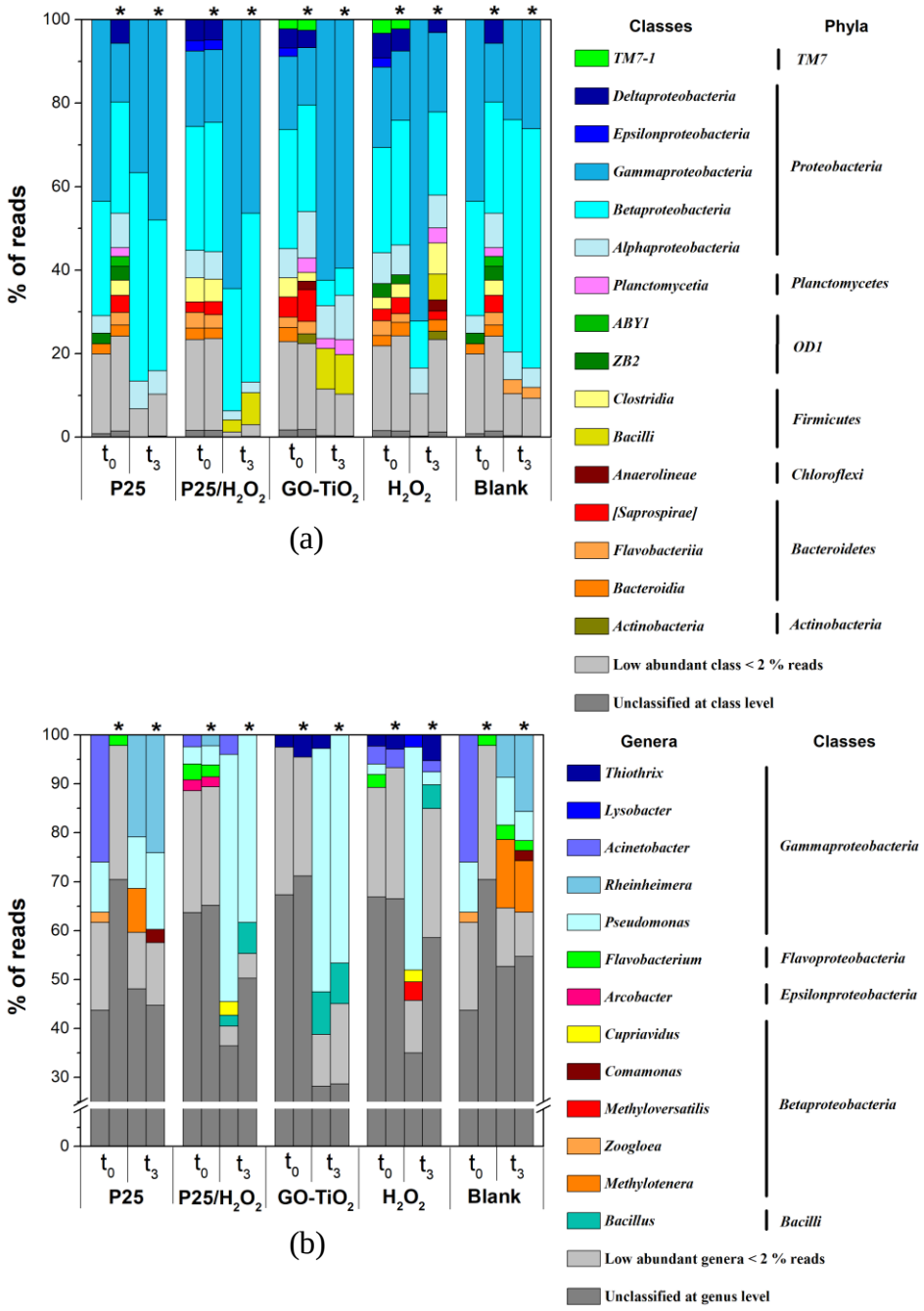

Figure 5. Relative abundance of (a) classes and (b) genera before (t_0) and 3-days after treatment (t_3). *, indicates a second independent assay.

Differences on the structure and composition of the bacterial community of the stored treated wastewater samples were mainly based on the relative abundance of *Beta-* and *Gammaproteobacteria* and *Bacilli* (Figs. 5a, t3 and Fig. 6, stars). The structure and composition of the bacterial communities of treated stored water was similar. Nevertheless, the relative abundance

of *Betaproteobacteria* was higher for photolysis > P25 > P25/H_2O_2 > solar-H_2O_2 > GO-TiO_2, varying between 57% and 7% (Fig. 5a). Consequently, the relative abundance of *Gammaproteobacteria* followed a kind of inverse order (i.e., GO-TiO_2 > P25/H_2O_2 > P25 > solar-H_2O_2 > photolysis), varying between 61% and 25% (Fig 5a). Despite the lower values when compared with these proteobacterial classes, the relative abundance of *Bacilli* followed a similar order (8% and 0%) (Fig.5a). The ability of members of class *Bacilli* to survive under harsh stressful conditions through the production of resistance forms (endospores) as well as their ability to withstand oxidative stress (Battistuzzi and Hedges 2009, Mols and Abee 2011) may explain their survival upon these treatments.

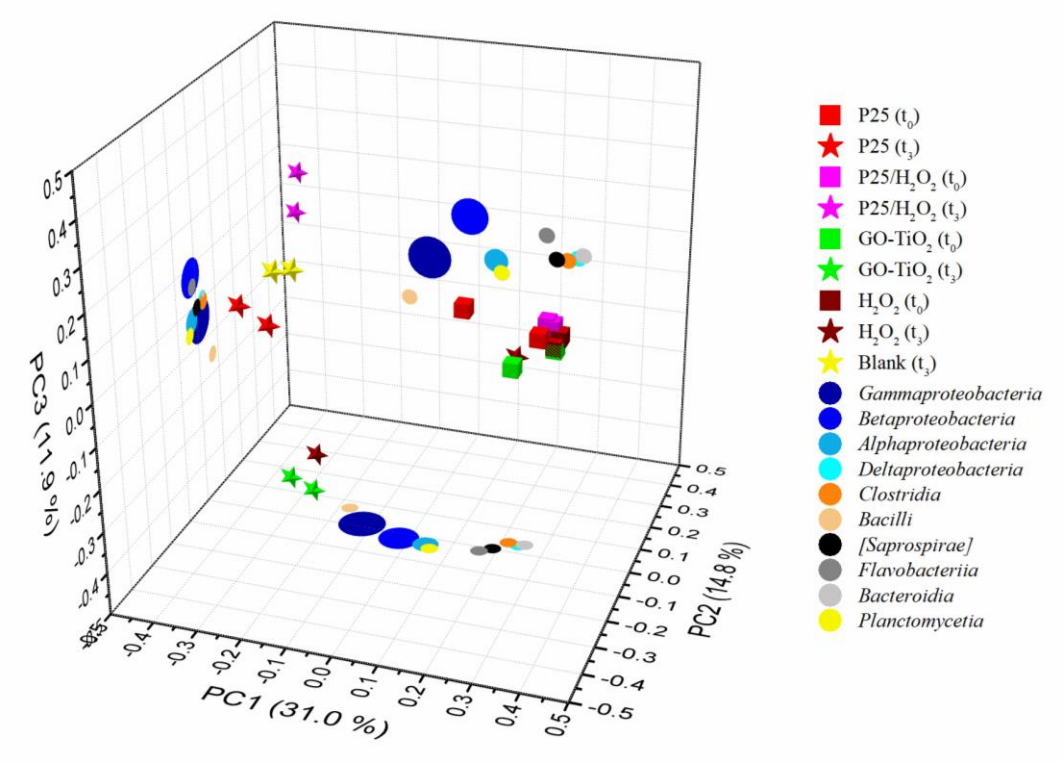

Figure 6. Biplot of principal coordinates analysis (PCoA) based on weighted Unifrac distances of samples before (t_0 - squares) and 3-days storage after treatment (t_3 – stars).

Altogether, the results obtained suggest that the solar-driven AOPs inactivated less efficiently *Beta-* and/or *Gammaproteobacteria* or that bacteria belonging to these classes have higher capacity to

446 regrow. Curiously, at the genus level, it is possible to observe that members of the ubiquitous genus
447 *Pseudomonas* were, in general, the group with the sharpest increase during storage, followed by
448 *Rheinheimera* and *Methilotenera* (Fig. 5b). Alterations in the composition and structure of the
449 bacterial communities leading to higher proportions of *Proteobacteria* in stored water than before
450 the treatment were reported in the literature for photolysis, ozonation and photocatalytic ozonation
451 (Becerra-Castro et al. 2016), coupled biological and photocatalysis treatments (Chen et al. 2013)
452 and ozonation coupled to a sequencing batch biofilm reactor (Esplugas et al. 2013).
453
454 **Conclusions**
455 Among the tested solar-driven oxidation processes, photo-Fenton at circumneutral pH was the
456 worst performing one (quite similar to photolysis), whereas the combination of P25 and H_2O_2 was
457 the most efficient approach for the removal of organic micropollutants in the urban wastewater
458 sampled.
459 Regarding the biological indicators, a decrease in the abundance of total faecal coliforms and
460 enterococci and their antibiotic resistant counterparts was found for all the processes employing
461 H_2O_2, which was permanent after 3-days storage of the treated wastewater. P25/H_2O_2 and solar-
462 H_2O_2 were also able to reduce the total bacterial load, assessed based on the abundance of the 16S
463 rRNA gene. Nevertheless, the abundance of total bacterial load increased after 3-days storage to
464 values close or higher than those verified before treatment. Similar observations were found for the
465 genes *intI1* and *sul1*. Hence, none of the studied processes was able to prevent bacterial
466 reactivation, including antibiotic resistant populations.
467 Thus, among all the studied processes, P25/H_2O_2 seemed to be that achieving the best compromise
468 for the removal of both organic micropollutants and biological contaminants, although not able to
469 prevent bacterial reactivation.
470 Interestingly, regardless of the oxidation process studied, higher relative abundance of the phylum
471 *Proteobacteria (Beta- and Gammaproteobacteria)*, namely of genera *Pseudomonas*, *Rheinheimera*

and *Methylotenera*, was observed in treated wastewater after 3-days storage. Since within the phylum *Proteobacteria*, in particular of the classes *Beta- and Gammaproteobacteria*, it is possible to find diverse multidrug-resistant bacteria, the increase of this group of organisms in stored treated water may deserve further investigation. Moreover, the potential disturbance of the water bacterial communities may have relevant ecology implication and should be considered in the design of advanced oxidation technologies.

Acknowledgments

This work was financially supported by Project nº P1404290052 under the SFERA Program (EC/FP7 - Integrating Activities), Project POCI-01-0145-FEDER-006984 – Associate Laboratory LSRE-LCM (UID/EQU/50020/2013) and POCI-01-0145-FEDER-006939 (LEPABE – UID/EQU/00511/2013), funded by FEDER through COMPETE2020 - Programa Operacional Competitividade e Internacionalização (POCI) – and by national funds through FCT - Fundação para a Ciência e a Tecnologia; UID/Multi/50016/2013-CBQF and Water JPI/0001/2013 STARE, and partially co-financed by QREN, ON2, FCT and FEDER through project AIProcMat@N2020 NORTE-01-0145-FEDER-000006, NORTE-07-0162-FEDER-000050 and NORTE-01-0145-FEDER-000005 (LEPABE-2-ECO-INNOVATION), supported by North Portugal Regional Operational Program (NORTE 2020), under the Portugal 2020 Partnership Agreement, through the ERDF. NFFM, LMPM and AMTS acknowledge PD/BD/114318/2016, IF/01248/2014 and IF/01501/2013, respectively. The authors would like to acknowledge the financial support provided by COST-European Cooperation in Science and Technology, to the COST Action ES1403: New and emerging challenges and opportunities in wastewater reuse (NEREUS). Disclaimer: The content of this article is the authors' responsibility and neither COST nor any person acting on its behalf is responsible for the use, which might be made of the information contained in it.

References

498 Fatta-Kassinos, D., Kalavrouziotis, I.K., Koukoulakis, P.H. and Vasquez, M.I. (2011) The risks
499 associated with wastewater reuse and xenobiotics in the agroecological environment. Science of
500 The Total Environment 409, 3555-3563.
501 Manaia, C.M., Macedo, G., Fatta-Kassinos, D. and Nunes, O.C. (2016) Antibiotic resistance in
502 urban aquatic environments: can it be controlled? Applied Microbiology and Biotechnology 100,
503 1543-1557.
504 Rizzo, L., Manaia, C., Merlin, C., Schwartz, T., Dagot, C., Ploy, M.C., Michael, I. and Fatta-
505 Kassinos, D. (2013) Urban wastewater treatment plants as hotspots for antibiotic resistant bacteria
506 and genes spread into the environment: A review. Science of The Total Environment 447, 345-360.
507 Ferro, G., Guarino, F., Castiglione, S. and Rizzo, L. (2016) Antibiotic resistance spread potential
508 in urban wastewater effluents disinfected by UV/H_2O_2 process. Science of The Total Environment
509 560–561, 29-35.
510 Davison, J. (1999) Genetic Exchange between Bacteria in the Environment. Plasmid 42, 73-91.
511 Ribeiro, A.R., Nunes, O.C., Pereira, M.F.R. and Silva, A.M.T. (2015) An overview on the
512 advanced oxidation processes applied for the treatment of water pollutants defined in the recently
513 launched Directive 2013/39/EU. Environment International 75, 33-51.
514 Moreira, N.F.F., Sousa, J.M., Macedo, G., Ribeiro, A.R., Barreiros, L., Pedrosa, M., Faria, J.L.,
515 Pereira, M.F.R., Castro-Silva, S., Segundo, M.A., Manaia, C.M., Nunes, O.C. and Silva, A.M.T.
516 (2016) Photocatalytic ozonation of urban wastewater and surface water using immobilized TiO_2
517 with LEDs: Micropollutants, antibiotic resistance genes and estrogenic activity. Water Research
518 94, 10-22.
519 Malato, S., Fernández-Ibáñez, P., Maldonado, M.I., Blanco, J. and Gernjak, W. (2009)
520 Decontamination and disinfection of water by solar photocatalysis: Recent overview and trends.
521 Catalysis Today 147, 1-59.
522 Sousa, J.M., Macedo, G., Pedrosa, M., Becerra-Castro, C., Castro-Silva, S., Pereira, M.F.R., Silva,
523 A.M.T., Nunes, O.C. and Manaia, C.M. (2017) Ozonation and $UV_{254\ nm}$ radiation for the removal

524 of microorganisms and antibiotic resistance genes from urban wastewater. Journal of Hazardous
525 Materials 323, 434-441.
526 Polo-López, M.I., Castro-Alférez, M., Oller, I. and Fernández-Ibáñez, P. (2014) Assessment of
527 solar photo-Fenton, photocatalysis, and H_2O_2 for removal of phytopathogen fungi spores in
528 synthetic and real effluents of urban wastewater. Chemical Engineering Journal 257, 122-130.
529 Pablos, C., Marugán, J., van Grieken, R. and Serrano, E. (2013) Emerging micropollutant oxidation
530 during disinfection processes using UV-C, UV-C/H_2O_2, UV-A/TiO_2 and UV-A/TiO_2/H_2O_2. Water
531 Research 47, 1237-1245.
532 Yang, W., Zhou, H. and Cicek, N. (2014) Treatment of organic micropollutants in water and
533 wastewater by UV-based processes: a literature review. Critical Reviews in Environmental Science
534 and Technology 44, 1443-1476.
535 Dunlop, P.S.M., Sheeran, C.P., Byrne, J.A., McMahon, M.A.S., Boyle, M.A. and McGuigan, K.G.
536 (2010) Inactivation of clinically relevant pathogens by photocatalytic coatings. Journal of
537 Photochemistry and Photobiology A: Chemistry 216, 303-310.
538 Ferro, G., Polo-López, M.I., Martínez-Piernas, A.B., Fernández-Ibáñez, P., Agüera, A. and Rizzo,
539 L. (2015) Cross-Contamination of Residual Emerging Contaminants and Antibiotic Resistant
540 Bacteria in Lettuce Crops and Soil Irrigated with Wastewater Treated by Sunlight/H_2O_2.
541 Environmental Science & Technology 49, 11096-11104.
542 Fiorentino, A., Ferro, G., Alferez, M.C., Polo-López, M.I., Fernández-Ibañez, P. and Rizzo, L.
543 (2015) Inactivation and regrowth of multidrug resistant bacteria in urban wastewater after
544 disinfection by solar-driven and chlorination processes. Journal of Photochemistry and
545 Photobiology B: Biology 148, 43-50.
546 Becerra-Castro, C., Macedo, G., Silva, A.M.T., Manaia, C.M. and Nunes, O.C. (2016)
547 Proteobacteria become predominant during regrowth after water disinfection. Science of The Total
548 Environment 573, 313-323.

549 Pastrana-Martínez, L.M., Morales-Torres, S., Likodimos, V., Figueiredo, J.L., Faria, J.L., Falaras,
550 P. and Silva, A.M.T. (2012) Advanced nanostructured photocatalysts based on reduced graphene
551 oxide–TiO_2 composites for degradation of diphenhydramine pharmaceutical and methyl orange
552 dye. Applied Catalysis B: Environmental 123, 241-256.
553 Rodríguez-Chueca, J., Polo-López, M.I., Mosteo, R., Ormad, M.P. and Fernández-Ibáñez, P.
554 (2014) Disinfection of real and simulated urban wastewater effluents using a mild solar photo-
555 Fenton. Applied Catalysis B: Environmental 150–151, 619-629.
556 Booshehri, A.Y., Polo-Lopez, M.I., Castro-Alférez, M., He, P., Xu, R., Rong, W., Malato, S. and
557 Fernández-Ibáñez, P. (2017) Assessment of solar photocatalysis using Ag/$BiVO_4$ at pilot solar
558 Compound Parabolic Collector for inactivation of pathogens in well water and secondary effluents.
559 Catalysis Today 281, 124-134.
560 Malato, S., Fernández-Ibáñez, P., Maldonado, M.I. and Oller, I. (2013) New and Future
561 Developments in Catalysis, pp. 371-393, Elsevier, Amsterdam.
562 Fernández-Ibáñez, P., Malato, S. and de las Nieves, F.J. (1999) Relationship between TiO_2 particle
563 size and reactor diameter in solar photoreactors efficiency. Catalysis Today 54(2), 195-204.
564 Barbosa, M.O., Moreira, N.F.F., Ribeiro, A.R., Pereira, M.F.R. and Silva, A.M.T. (2016)
565 Occurrence and removal of organic micropollutants: An overview of the watch list of EU Decision
566 2015/495. Water Research 94, 257-279.
567 Polo-López, M.I., Fernández-Ibáñez, P., Ubomba-Jaswa, E., Navntoft, C., García-Fernández, I.,
568 Dunlop, P.S.M., Schmid, M., Byrne, J.A. and McGuigan, K.G. (2011) Elimination of water
569 pathogens with solar radiation using an automated sequential batch CPC reactor. Journal of
570 Hazardous Materials 196, 16-21.
571 Narciso-da-Rocha, C., Varela, A.R., Schwartz, T., Nunes, O.C. and Manaia, C.M. (2014) *blaTEM*
572 and *vanA* as indicator genes of antibiotic resistance contamination in a hospital–urban wastewater
573 treatment plant system. Journal of Global Antimicrobial Resistance 2, 309-315.

574 Denman, S.E. and McSweeney, C.S. (2006) Development of a real-time PCR assay for monitoring
575 anaerobic fungal and cellulolytic bacterial populations within the rumen. FEMS Microbiology
576 Ecology 58, 572-582.
577 Bibbal, D., Dupouy, V., Ferré, J.P., Toutain, P.L., Fayet, O., Prère, M.F. and Bousquet-Mélou, A.
578 (2007) Impact of three ampicillin dosage regimens on selection of ampicillin resistance in
579 Enterobacteriaceae and excretion of blaTEM genes in swine feces. Applied and Environmental
580 Microbiology 73, 4785-4790.
581 Goldstein, C., Lee, M.D., Sanchez, S., Hudson, C., Phillips, B., Register, B., Grady, M., Liebert,
582 C., Summers, A.O., White, D.G. and Maurer, J.J. (2001) Incidence of class 1 and 2 integrases in
583 clinical and commensal bacteria from livestock, companion animals, and exotics. Antimicrobial
584 Agents and Chemotherapy 45, 723-726.
585 Marti, E. and Balcázar, J.L. (2013) Real-time PCR assays for quantification of qnr genes in
586 environmental water samples and chicken feces. Applied and Environmental Microbiology 79,
587 1743-1745.
588 Pei, R., Kim, S.C., Carlson, K.H. and Pruden, A. (2006) Effect of River Landscape on the sediment
589 concentrations of antibiotics and corresponding antibiotic resistance genes (ARG). Water Research
590 40, 2427-2435.
591 Volkmann, H., Schwartz, T., Bischoff, P., Kirchen, S. and Obst, U. (2004) Detection of clinically
592 relevant antibiotic-resistance genes in municipal wastewater using real-time PCR (TaqMan).
593 Journal of Microbiological Methods 56, 277-286.
594 Marti, E., Variatza, E. and Balcázar, J.L. (2014) Bacteriophages as a reservoir of extended-
595 spectrum β -lactamase and fluoroquinolone resistance genes in the environment. Clinical
596 Microbiology and Infection 20, O456-O459.
597 Caporaso, J.G., Kuczynski, J., Stombaugh, J., Bittinger, K., Bushman, F.D., Costello, E.K., Fierer,
598 N., Peña, A.G., Goodrich, J.K., Gordon, J.I., Huttley, G.A., Kelley, S.T., Knights, D., Koenig, J.E.,
599 Ley, R.E., Lozupone, C.A., McDonald, D., Muegge, B.D., Pirrung, M., Reeder, J., Sevinsky, J.R.,

600 Turnbaugh, P.J., Walters, W.A., Widmann, J., Yatsunenko, T., Zaneveld, J. and Knight, R. (2010a)
601 QIIME allows analysis of high-throughput community sequencing data. Nature methods 7, 335-
602 336.
603 Schmieder, R. and Edwards, R. (2011) Quality control and preprocessing of metagenomic datasets.
604 Bioinformatics 27, 863-864.
605 Edgar, R.C. (2010) Search and clustering orders of magnitude faster than BLAST. Bioinformatics
606 26, 2460-2461.
607 Caporaso, J.G., Bittinger, K., Bushman, F.D., DeSantis, T.Z., Andersen, G.L. and Knight, R.
608 (2010b) PyNAST: a flexible tool for aligning sequences to a template alignment. Bioinformatics
609 26, 266-267.
610 Shannon, C.E. and Weaver, W. (1963) The mathematical theory of communication, University of
611 Illinois Press, Urbana.
612 Simpson, E.H. (1949) Measurement of diversity. Nature 163, 688.
613 Faith, D.P. (1992) Conservation evaluation and phylogenetic diversity. Biological Conservation
614 61, 1-10.
615 Paulson, J.N., Stine, O.C., Bravo, H.C. and Pop, M. (2013) Differential abundance analysis for
616 microbial marker-gene surveys. Nat Meth 10, 1200-1202.
617 Lozupone, C. and Knight, R. (2005) UniFrac: a New Phylogenetic Method for Comparing
618 Microbial Communities. Applied and Environmental Microbiology 71, 8228-8235.
619 Parks, D.H., Tyson, G.W., Hugenholtz, P. and Beiko, R.G. (2014) STAMP: statistical analysis of
620 taxonomic and functional profiles. Bioinformatics 30, 3123-3124.
621 Moreira, N.F.F., Orge, C.A., Ribeiro, A.R., Faria, J.L., Nunes, O.C., Pereira, M.F.R. and Silva,
622 A.M.T. (2015) Fast mineralization and detoxification of amoxicillin and diclofenac by
623 photocatalytic ozonation and application to an urban wastewater. Water Research 87, 87-96.
624 Cruz, M., Gomez, C., Duran-Valle, C.J., Pastrana-Martínez, L.M., Faria, J.L., Silva, A.M.T.,
625 Faraldos, M. and Bahamonde, A. (2017) Bare TiO_2 and graphene oxide TiO_2 photocatalysts on the

626 degradation of selected pesticides and influence of the water matrix. Applied Surface Science 416,
627 1013-1021.
628 Sampaio, M.J., Silva, C.G., Silva, A.M.T., Pastrana-Martínez, L.M., Han, C., Morales-Torres, S.,
629 Figueiredo, J.L., Dionysiou, D.D. and Faria, J.L. (2015) Carbon-based TiO_2 materials for the
630 degradation of Microcystin-LA. Applied Catalysis B: Environmental 170–171, 74-82.
631 Maroga Mboula, V., Héquet, V., Andrès, Y., Pastrana-Martínez, L.M., Doña-Rodríguez, J.M.,
632 Silva, A.M.T. and Falaras, P. (2013) Photocatalytic degradation of endocrine disruptor compounds
633 under simulated solar light. Water Research 47, 3997-4005.
634 Kositzi, M., Poulios, I., Malato, S., Caceres, J. and Campos, A. (2004) Solar photocatalytic
635 treatment of synthetic municipal wastewater. Water Research 38, 1147-1154.
636 Xing, W., Lalwani, G., Rusakova, I. and Sitharaman, B. (2014) Degradation of graphene by
637 hydrogen peroxide. Particle & Particle Systems Characterization 31, 745-750.
638 Giannakis, S., Hendaoui, I., Rtimi, S., Fürbringer, J.-M. and Pulgarin, C. (2017) Modeling and
639 treatment optimization of pharmaceutically active compounds by the photo-Fenton process: The
640 case of the antidepressant Venlafaxine. Journal of Environmental Chemical Engineering 5, 818-
641 828.
642 Agulló-Barceló, M., Polo-López, M.I., Lucena, F., Jofre, J. and Fernández-Ibáñez, P. (2013) Solar
643 advanced oxidation processes as disinfection tertiary treatments for real wastewater: implications
644 for water reclamation. Applied Catalysis B: Environmental 136, 341-350.
645 García-Fernández, I., Polo-López, M.I., Oller, I. and Fernández-Ibáñez, P. (2012) Bacteria and
646 fungi inactivation using Fe3+/sunlight, H2O2/sunlight and near neutral photo-Fenton: A
647 comparative study. Applied Catalysis B: Environmental 121, 20-29.
648 Aguas, Y., Hincapie, M., Fernández-Ibáñez, P. and Polo-López, M.I. (2017) Solar photocatalytic
649 disinfection of agricultural pathogenic fungi (Curvularia sp.) in real urban wastewater. Science of
650 The Total Environment 607, 1213-1224.

651 Castro-Alférez, M., Polo-López, M.I., Marugán, J. and Fernández-Ibáñez, P. (2017) Mechanistic
652 modeling of UV and mild-heat synergistic effect on solar water disinfection. Chemical Engineering
653 Journal 316, 111-120.
654 Polo-López, M.I., Castro-Alférez, M., Nahim-Granados, S., Malato, S. and Fernández-Ibáñez, P.
655 (2017) Legionella jordanis inactivation in water by solar driven processes: EMA-qPCR versus
656 culture-based analyses for new mechanistic insights. Catalysis Today 287, 15-21.
657 Sichel, C., Fernández-Ibáñez, P., de Cara, M. and Tello, J. (2009) Lethal synergy of solar UV-
658 radiation and H_2O_2 on wild *Fusarium solani* spores in distilled and natural well water. Water
659 Research 43, 1841-1850.
660 Polo-López, M.I., Oller, I. and Fernández-Ibáñez, P. (2013) Benefits of photo-Fenton at low
661 concentrations for solar disinfection of distilled water. A case study: *Phytophthora capsici*.
662 Catalysis Today 209, 181-187.
663 Cruz-Ortiz, B.R., Hamilton, J.W.J., Pablos, C., Díaz-Jiménez, L., Cortés-Hernández, D.A.,
664 Sharma, P.K., Castro-Alférez, M., Fernández-Ibañez, P., Dunlop, P.S.M. and Byrne, J.A. (2017)
665 Mechanism of photocatalytic disinfection using titania-graphene composites under UV and visible
666 irradiation. Chemical Engineering Journal 316, 179-186.
667 Fernández-Ibáñez, P., Polo-López, M.I., Malato, S., Wadhwa, S., Hamilton, J.W.J., Dunlop,
668 P.S.M., D'Sa, R., Magee, E., O'Shea, K., Dionysiou, D.D. and Byrne, J.A. (2015) Solar
669 photocatalytic disinfection of water using titanium dioxide graphene composites. Chemical
670 Engineering Journal 261, 36-44.
671 Zhao, X., Hu, H.Y., Yu, T., Su, C., Jiang, H. and Liu, S. (2014) Effect of different molecular weight
672 organic components on the increase of microbial growth potential of secondary effluent by
673 ozonation. Journal of Environmental Sciences (China) 26, 2190-2197.
674 Spuhler, D., Andrés Rengifo-Herrera, J. and Pulgarin, C. (2010) The effect of Fe^{2+}, Fe^{3+}, H_2O_2 and
675 the photo-Fenton reagent at near neutral pH on the solar disinfection (SODIS) at low temperatures
676 of water containing *Escherichia coli* K12. Applied Catalysis B: Environmental 96(1–2), 126-141.

677 Ubomba-Jaswa, E., Navntoft, C., Polo-López, M.I., Fernandez-Ibáñez, P. and McGuigan, K.G.
678 (2009) Solar disinfection of drinking water (SODIS): An investigation of the effect of UV-A dose
679 on inactivation efficiency. Photochemical and Photobiological Sciences 8, 587-595.
680 Giannakis, S., Merino Gamo, A.I., Darakas, E., Escalas-Cañellas, A. and Pulgarin, C. (2014)
681 Monitoring the post-irradiation *E. coli* survival patterns in environmental water matrices:
682 Implications in handling solar disinfected wastewater. Chemical Engineering Journal 253, 366-
683 376.
684 Battistuzzi, F.U. and Hedges, S.B. (2009) A Major Clade of Prokaryotes with Ancient Adaptations
685 to Life on Land. Molecular Biology and Evolution 26, 335-343.
686 Mols, M. and Abee, T. (2011) Primary and secondary oxidative stress in Bacillus. Environmental
687 Microbiology 13, 1387-1394.
688 Chen, C.-Y., Kuo, J.-T., Yang, H.-A. and Chung, Y.-C. (2013) A coupled biological and
689 photocatalysis pretreatment system for the removal of crystal violet from wastewater.
690 Chemosphere 92, 695-701.
691 Esplugas, M., González, O. and Sans, C. (2013) Bacterial community characterization of a
692 sequencing batch reactor treating pre-ozonized sulfamethoxazole in water. Environmental
693 Technology 34, 1583-1591.
694